Journal of
Marine Science and Engineering

MDPI

Article

Study on the Mechanism of Natural Gas Hydrate Decomposition and Seabed Seepage Triggered by Mass Transport Deposits

Pengqi Liu [1,2], Wei Zhang [1,2,*], Shuang Mao [3,4,*], Pibo Su [1,2], Huaizhen Chen [5] and Liguo Hu [6]

1 Sanya Institute of South China Sea Geology, Guangzhou Marine Geological Survey, Sanya 572025, China; liupengqi@mail.cgs.gov.cn (P.L.); spb_525@sina.com (P.S.)
2 Academy of South China Sea Geological Science, China Geological Survey, Sanya 572025, China
3 Economics & Technology Research Institute of Liaohe Oilfield Company, PetroChina, Panjin 124000, China
4 School of Geosciences, Yangtze University, Wuhan 430100, China
5 State Key Laboratory of Marine Geology, School of Ocean and Earth Science, Tongji University, Shanghai 200092, China; huaizhenchen@tongji.edu.cn
6 PetroChina Liaohe Oilfield Company, Panjin 124010, China; hulg@petrochina.com.cn
* Correspondence: zwei_a@mail.cgs.gov.cn (W.Z.); ms1991@petrochina.com.cn (S.M.)

Abstract: Previous studies indicate that mass transport deposits are related to the dynamic accumulation of natural gas hydrates and gas leakage. This research aims to elucidate the causal mechanism of seabed seepage in the western region of the southeastern Qiongdongnan Basin through the application of seismic interpretation and attribute fusion techniques. The mass transport deposits, bottom simulating reflector, submarine mounds, and other phenomena were identified through seismic interpretation techniques. Faults and fractures were identified by utilizing variance attribute analysis. Gas chimneys were identified using instantaneous frequency attribute analysis. Free gas and paleo-seepage points were identified using sweetness attributes, enabling the analysis of fluid seepage pathways and the establishment of a seepage evolution model. Research has shown that in areas where the mass transport deposits develop thicker layers, there is a greater uplift of the bottom boundary of the gas hydrate stability zone, which can significantly alter the seafloor topography. Conversely, the opposite is true. The research indicates that the upward migration of the gas hydrate stability zone, induced by the mass transport deposits in the study area, can result in the rapid decomposition of gas hydrates. The gas generated from the decomposition of gas hydrates is identified as the principal factor responsible for inducing seabed seepage. Moderate- and low-speed natural gas seepage can create spiny seamounts and domed seamounts, respectively.

Keywords: Qiongdongnan Basin; gas hydrate; seafloor seepage mechanism; attribute analysis technology; the mass transported deposits; spiny seamounts; domed seamounts

check for updates

Citation: Liu, P.; Zhang, W.; Mao, S.; Su, P.; Chen, H.; Hu, L. Study on the Mechanism of Natural Gas Hydrate Decomposition and Seabed Seepage Triggered by Mass Transport Deposits. *J. Mar. Sci. Eng.* **2024**, *12*, 646. https://doi.org/10.3390/jmse12040646

Academic Editor: Atilla Incecik

Received: 10 February 2024
Revised: 28 March 2024
Accepted: 2 April 2024
Published: 12 April 2024

1. Introduction

Submarine gas seepage represents a ubiquitous and dynamic geological phenomenon within the marine environment. It involves the migration of various fluids, such as shallow gas, submarine groundwater, cold seep fluid, hydrothermal fluid, and liquefied fine-grained sediments. These fluids flow through predominant pathways, like faults, fractures, mud volcanoes, or gas chimneys beneath the seabed interface, eventually reaching their discharge or eruption on the ocean floor [1]. Such seepage occurrences have been documented across various marine environments, spanning passive and active continental margins, including the South China Sea, North Sea, Baltic Sea, Black Sea, North Atlantic, Gulf of Mexico, Sea of Japan, Japan Sea Trench, Mediterranean Sea, Indian Ocean, and Southwest Pacific [2–8].

The manifestation of submarine gas seepage is intricately linked to geological processes and is influenced by factors, such as rapid sedimentation, tectonic uplift, erosion, faulting, and hydrate decomposition [9–12]. During periods of rapid sedimentation, substantial sediment accumulation can result in the formation of thick subsurface layers. This can lead to elevated pore water pressure and the subsequent migration of pre-existing subsurface fluids due to compaction-related compression. Tectonic uplift and erosion have complex effects on the migration of subsurface fluids, altering flow paths and velocities, and impacting storage and migration processes [13,14]. Faulting can disrupt upper fluid seals, which can facilitate vertical fluid migration [15]. Submarine gas seepage serves as an indicator of the presence of natural gas hydrates and hydrocarbon accumulations within sedimentary layers. In regions with intense gas seepage, high gas hydrate saturation is often observed on or below the seabed [16]. Additionally, gas hydrates may contribute to geological formation fracturing, further promoting submarine seepage occurrences [17,18]. Such seepage events significantly modify seafloor topography and geomorphology, giving rise to various submarine micro-landform types, including pockmarks, authigenic carbonate crusts, spiny seamounts, domed seamounts, and mud volcanoes [19].

The research focus area is located within the deepwater region of the northern South China Sea continental slope. Previous studies have investigated submarine micro-landforms and fluid seepage in this area, uncovering various types of micro-landforms, such as pockmarks, spiny seamounts, and domed seamounts. Marine geological investigations over several years have established a close correlation between submarine micro-landform formation, gas hydrate formation, and decomposition, in addition to the widespread development of the mass transport deposit (MTD) systems [20]. However, current research inadequately examines the causal mechanisms of submarine seepage involving hydrates and MTDs. This study aims to explore the interrelationships among natural gas hydrates, submarine micro-landforms, and MTD sedimentary systems, elucidating their impacts on submarine gas seepage mechanisms, particularly focusing on the influence of MTDs on hydrate decomposition and seafloor seepage intensity.

Methodologically, this study employs variance attribute volume, sweetness attribute volume, and instantaneous frequency attribute volume fusion analysis techniques to identify geological phenomena, such as MTDs, bottom simulating reflectors (BSRs), spiny seamounts, fault systems, gas chimneys, and paleo-seepage points. Through relational analysis, a unique model for the evolution of seafloor fluid seepage specific to the study area is proposed. This contributes to a deeper understanding of seafloor geomorphology formation, evolution, and fluid seepage mechanisms.

This study utilizes seismic attribute fusion technology to assess the influence of MTDs on the gas hydrate stability zone, uncovering their effects on submarine natural gas seepage and micro-landforms. Additionally, a unique fluid seepage genesis model specific to the study area is proposed, expanding upon previous research that focused solely on the impact of MTDs on subsurface fluids. References remain unchanged.

2. Geologic Setting, Data, and Method

The Qiongdongnan Basin (QDNB) is located in the northwestern part of the South China Sea, to the southeast of Hainan Island, and extends in the NEE direction. It is considered a Cenozoic extensional basin developed over strongly thinned continental crust and is a significant oil and gas, as well as natural gas, hydrate basin [21]. The study area is situated in a tectonically gentle region between the continental slope and the uplifted platform, and the topography is relatively flat (Figure 1).

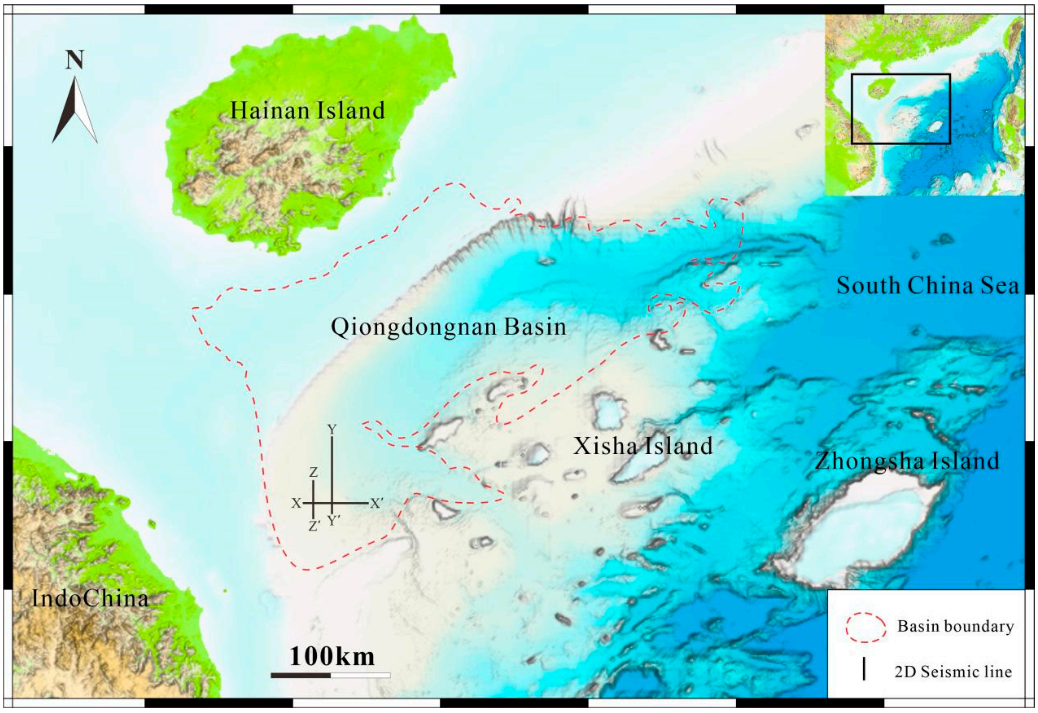

Figure 1. Regional location map of the study area. The red dashed line represents the boundary of the QDNB. The black line segments represent the positions of seismic profiles.

The sedimentary fill during the tectonic rifting period in the study area comprises three stratigraphic units: the Eocene, Yacheng Formation, and Lingshui Formation. The sedimentary transition from continental to shallow marine facies is characterized by the development of fan-deltas and deltas. During the faulting period, the sedimentary fill includes the Miocene Lingshui Formation Member 1–2, the Lower-Middle Miocene Sanya Formation, and the Meishan Formation. The sedimentation gradually transitions from shallow marine to semi-deep marine, featuring the development of deltas, fan-deltas, and platform-margin reefs, among other features. During the subsidence stage, the sedimentary fill includes the Upper-Middle Miocene Huangliu Formation, Upper Miocene Yinggehai Formation, and Quaternary Ledong Formation. These sediments were deposited in a semi-deep marine environment and are characterized by gravity flow deposits, such as debris flows, turbidite fans, slope apron fans, and canyon channels (See Figure 2) [22,23].

The target interval of this study is the Quaternary Leidong Formation (Figure 2). Within this formation, there is significant variation in sediment thickness. The sedimentary thickness is greater in the northwest direction, with a maximum sedimentation rate reaching up to 550 m per million years. In contrast, the sedimentary thickness is thinner in the southeast direction, with a sedimentation rate of only 50 m per million years. The sedimentary strata in the northwest direction are influenced by the influx of materials from the continental slope. During the lowstand and transgression periods, debris flow and turbidite deposits are developed, mainly comprising slope fans, basin floor fans, channel-levee systems, and MTDs that rapidly accumulate [24]. During the highstand system tract, the depositional environment transitions to a low-energy, fine-grained settling sedimentation in a semi-deep sea setting. In the southeast direction, the sedimentary strata are mainly influenced by slow sedimentation during the subsidence stage, resulting in semi-deep marine deposition. The hydrodynamic conditions are relatively weak, creating a stable semi-deep marine depositional environment. The study area contains four sets of SR pods: the Yacheng Formation, the LingShui Formation Member 3, the LingShui Formation Member 1–2, the Meishan Formation, and the Huangliu Formation. Among them, the LingShui Formation Member 3 and the LingShui Formation Member 1–2 in the Meishan Formation are the main gas source layers for gas hydrates [25].

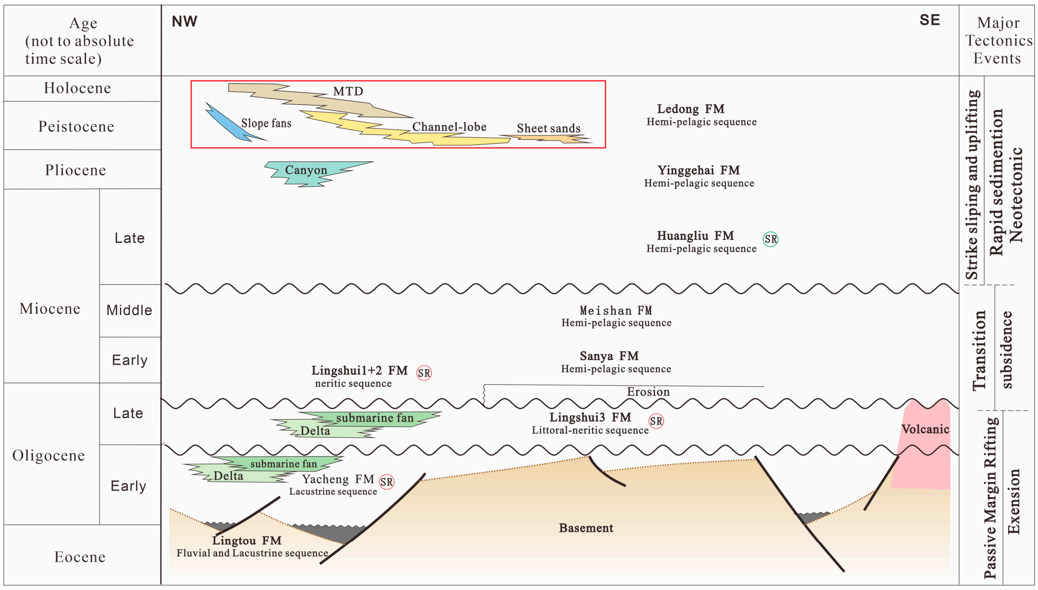

Figure 2. The simplified diagram illustrating the sedimentary facies, lithology, and regional tectonic movements from the Paleogene to the Quaternary in the study area. The red rectangular box represents the target interval of the study. Within this interval, the red circles labeled as "SR" denote thermogenic gas source rocks, while the green circles labeled as "SR" represent biogenic gas source rocks.

3. Data and Method

The seismic volume covers a surface area of 2900 km^2 and has a total trace length of 7 s TWT. The bin spacing is 12.5 m in both directions with a sample rate of 2 ms TWT. The seismic volume is a full-offset, post-stack time migrated (PSTM) volume. Processing steps included signal noise reduction, corrections, and velocity analysis using Kirchhoff PSTM. Noise removal is carried out within the frequency range of 10 Hz to 20 Hz. The resolution of seismic data depends on the dominant frequency of the seismic signal and the interval velocity in the zone of interest. The interval velocity of the sediment package containing mounds and domes is approximately 0.7 km/ms, as determined from velocity data obtained through the well-to-seismic correlation within the 2D seismic volume.

When the subsurface contains fluids, it can affect the amplitude, frequency, and energy of seismic waves, thereby causing post-stack attribute anomalies in seismic data. To identify and analyze geological factors, such as free gas, faults, and fractures, a combination of attributes, like instantaneous frequency, sweetness, and variance, can be selected. The instantaneous frequency refers to the derivative of the instantaneous phase with respect to time [26,27]. The main factors causing variations in instantaneous frequency values include changes in lithology, properties of the fillings within the strata, and lateral heterogeneity in distribution [28]. The presence of free gas in pores within the strata can lead to high-frequency attenuation and low-frequency enhancement effects. In this study, the instantaneous frequency within the frequency range of 13 Hz to 28 Hz was chosen as a sensitive attribute to reflect the spatial distribution characteristics of gas-bearing formations. The reason for choosing this range is that it effectively reflects the developmental range of subsurface fluids. The sweetness attribute is the ratio of seismic amplitude to the square root of the instantaneous frequency. Methane fluid seepage is often accompanied by phenomena, such as authigenic carbonate crusts and chemosynthetic biogenic shells. These occurrences result in high-amplitude anomalies, leading to high values of the sweetness attribute. This attribute plays a crucial role in identifying both present-day seepage sites and ancient seepage points on the seabed [29]. The variance attribute is used to describe the lateral heterogeneity of seismic properties, such as lithology and stratigraphy, by utilizing the similarity between adjacent seismic traces [30]. It can reveal the discontinuous information within the data volume and characterize fault systems. This study primarily utilizes the multi-attribute fusion technique to analyze the source-sink system of natural gas hydrate mineralization. This approach reduces the uncertainties caused by interpreting a single data volume and highlights abundant geological information, thereby enhancing the reliability of geological understanding. The accuracy of individual seismic attributes in the geological interpretation and comprehensive evaluation may be subject to uncertainties. Conducting geological interpretation through the simultaneous use of multiple attributes significantly reduces ambiguity, thereby enhancing the reliability of the geological understanding.

4. Results

In Figure 3A, on the left side, there are submarine spiny seamounts developed on the seafloor, while on the right side, there is a submarine domed seamount. On the whole, the Huangliu Formation, Yinggehai Formation, and Ledong Formation, situated below the two geological bodies, exhibit significant low-frequency anomalies, along with the presence of gas chimney structures. It is inferred that there is a substantial amount of gas in the strata, with the spiky mounds corresponding to a higher gas content. Coherent body anomalies can indicate the development of faults. From the figure, it can be observed that the area corresponding to the spiny mounds shows the development of faults throughout the seabed to the Huangliu Formation, with the fractures being most pronounced in the Yinggaohai Formation. The domed seamount also exhibits faults extending from the seabed to the Yinggaohai Formation, but the fracture density is lower compared to the spiny seamounts. These fractures serve as conduits for gas migration. The spiny seamounts exhibit anomalies in the sweetness attribute on the seabed, while sporadic anomalies are observed in the sweetness attribute of the underlying strata of the MTDs. The domed seamount shows no anomalies of sweetness attributes on the seabed, but distinct scattered anomalies are present in the underlying strata of the MTDs. The Yinggaohai Formation exhibits localized anomalies in sweetness attributes. These anomalies could be attributed to the presence of gas-rich formations or the occurrence of seafloor seepage points (both current and ancient), which might have led to the formation of authigenic carbonate concretions and chemo-bio shells in the vicinity. From the local zoom-in of Figure 3A (Figure 3B), it can be observed that sporadic BSR occurrences develop near the base of the gas hydrate stability zone (BGHSZ) corresponding to the domed seamount, while no apparent BSR phenomenon is observed near BGHSZ corresponding to the spiny seamounts. Profile YY′ intersects with profile XX′ at point N. In the vicinity of the intersection point on profile YY′ (within the yellow box in Figure 3B), the BSR phenomenon is observed near the BGHSZ. However, in the vicinity of the intersection point on profile XX′ (within the yellow box in Figure 3D), the BSR is even more pronounced. Profile YY′ intersects with profile ZZ′ at point M. Both profiles show clear BSR phenomena in the vicinity of the intersection point within the BHSZ (Figure 3C,D). At the intersection point on profile ZZ′, there is a distinct presence of a domed seamount on the seafloor. The Ledong Formation contains two stages of MTDs (MTD1 and MTD2). As shown in Figure 3B, both stages of massive sulfide deposits (MTDs) exhibit thicker accumulations on the spiny seamounts compared to the domed seamounts. Based on the paleostatic conditions of the study area, MTD1 and MTD2 correspond to the paleo-base of the gas hydrate stability zone (Pelo-BGHSZ1 and Pelo-BGHSZ2, respectively, as indicated in the figure). Furthermore, the paleo-BHSZ intersects with anomalies in the sweetness attribute. The base map in Figure 3E displays the combined thickness of MTD1 and MTD2. The white dashed line delineates the development zone of spiny seamounts, while the black dashed line marks the development zone of domed seamounts. It can be observed that the spiny seamount development zone exhibits thicker MTDs, while the domed seamount development zone shows thinner MTDs.

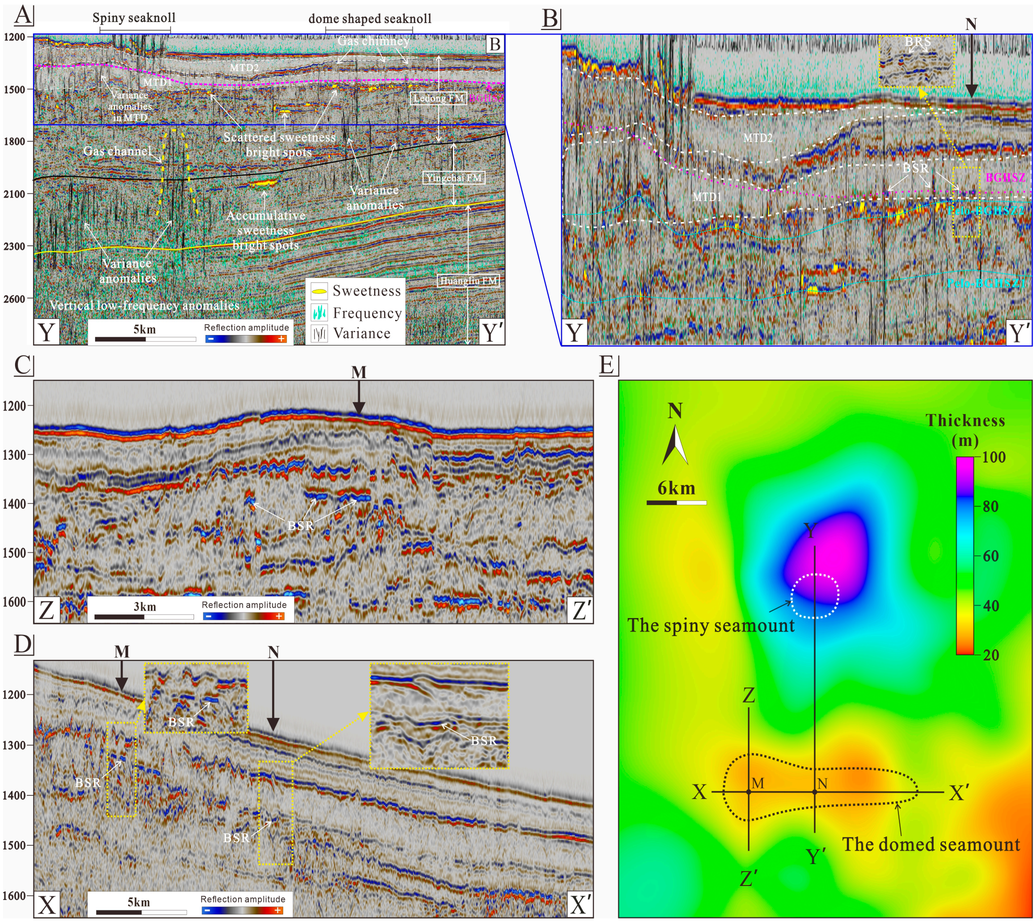

Figure 3. (**A**) The superimposed seismic profiles of the seismic data, instantaneous dominant frequency attribute, variance attribute, and sweetness attribute in the research area. The white dashed circles indicate MTDs, the yellow dashed lines represent gas chimney outlines, the pink dashed line represents the present-day BGHSZ, the bright green color represents the instantaneous dominant frequency attribute values in the range of 13 to 28 Hz, the black vertical lines indicate high-value anomalies in the variance attribute, and the yellow color represents data with sweetness attribute values above 5000. (**B**) The enlarged view of the blue-boxed region in (**A**). The light blue dashed line represents the paleo base of the gas hydrate stability zone. (**C**) The seismic profile at position Z-Z′ in (**E**). (**D**) The seismic profile at position X-X′ in (**E**). (**E**) The map indicating the positions of the seismic profiles. The base map color represents the sum of MTD1 and MTD2 thicknesses, the white dashed line represents the development range of spiny seamounts, the black dashed line represents the development range of domed seamount, and M and N points are the intersections of seismic lines.

5. Discussions

5.1. Mechanism of Hydrate Decomposition Induced by MTDS

The formation of gas hydrates requires appropriate temperature and pressure conditions. Lower temperatures and higher pressures facilitate the formation of hydrogen bonds between water molecules and natural gas molecules, leading to the formation of stable gas hydrate structures that prevent the escape of natural gas molecules. Additionally, the formation of gas hydrates involves nucleation and growth processes. Under suitable temperature and pressure conditions, water and gas molecules can form initial gas hydrate structures through a process known as nucleation. Over time, more water and gas molecules are adsorbed and incorporated into the existing nuclei, forming larger gas hydrate crystals, a process known as growth. This process requires suitable temperature and pressure conditions to ensure adequate energy and stability.

MTDs are widely distributed in various settings, such as outer continental shelves, upper continental slopes, canyons, uplifts (volcanoes, ridges, salt domes), and sidewalls of channels. They are commonly found in deepwater basins globally and typically form during sea-level falls. Previous studies suggest that the rapid deposition of MTDs can cause rapid changes in the temperature and pressure conditions within their coverage areas. This leads to a significant uplift in the gas hydrate stability zone boundary, resulting in the rapid decomposition of pre-existing gas hydrates.

Submarine mound features in the study area are primarily distributed in regions with high Quaternary sedimentation rates and thick accumulations of MTDs. On seismic profiles, these features exhibit distinct "spike" shapes. These development areas of submarine mound features are accompanied by extensive seafloor sediment folding phenomena. Submarine domed seamounts are mainly distributed in areas with smaller Quaternary sediment thickness and smaller thicknesses of MTDs. On seismic profiles, they exhibit gentle positive uplift slopes. As the thickness of MTDs increases, their impact on the gas hydrate stability zone boundary becomes more significant. Therefore, compared to domed seamounts, the influence of MTDs corresponding to spiny seamounts is greater on the stability zone boundary, leading to a higher intensity of gas hydrate decomposition.

The influence of MTDs on the temperature and pressure conditions of gas hydrates can result in the upward movement of the gas hydrate stability zone boundary, leading to the decomposition of pre-existing gas hydrates. Subsequently, the decomposed gas can reform gas hydrate deposits within new suitable stability zones, thereby affecting the distribution patterns and formation mechanisms of gas hydrate deposits.

5.2. The Geological Effects Caused by Hydrate Decomposition

The decomposition of natural gas hydrates yields a significant volume of gas, which rises and creates fractures. These fractures act as preferential conduits for the upward migration of free gas. In regions abundant in gas supply, these fractures continue to propagate upwards, facilitating gas seepage toward the seafloor.

The formation of hydrates induces sediment expansion and carbonate precipitation around seafloor seepage sites, leading to the formation of submarine spiny seamounts. These seamount features arise from the accumulation of free gas within sedimentary layers. The gas displaces water in the upper sediment pores, causing localized expansion and forming positive topographic uplifts [31]. An analysis of the instantaneous frequency attribute in Figure 3A reveals that the development of submarine spiny seamount areas signifies a higher gas supply, which can stimulate persistent and rapid gas seepage on the seafloor, consequently leading to ongoing destabilization of the shallow sediment. This phenomenon likely contributes significantly to the chaotic seismic imaging and prominent manifestation of seafloor gas seepage in the underlying sedimentary layers of the submarine mound features.

The thickness of MTDs is relatively thin in the wing areas, resulting in a comparatively smaller uplift of the BGHSZ in the MTDs' wing coverage regions. The gas formed by the decomposition of natural gas hydrates can be rapidly trapped within the newly formed hydrate stability zone. This process leads to the creation of new natural gas hydrate deposits, which, in turn, hinder the upward development of fractures. In these regions, strong seabed seepage is usually not present. The sediment expansion caused by the formation of hydrates can create submarine domed seamount features on the seabed. The formation of submarine domed seamounts is similar to that of spiny seamount structures. Both result from the displacement of water in the pore space of overlying sediment by leaking gas, causing localized expansion of the sediment volume. In most cases, submarine domed seamounts are situated directly above gas-rich layers and typically only rise a few meters above the normal seabed, but their spans can extend up to several hundred meters [32].

In their study on the seabed gas seepage characteristics in the northern Gulf of Mexico continental slope, Roberts et al. found that moderate-velocity natural gas seepage can lead to the formation of gas hydrate mounds, isolated authigenic carbonate mounds, and small cold seeps on the seafloor [33]. Low-velocity natural gas seepage, on the other hand, is more likely to result in the formation of authigenic carbonate mounds, hardgrounds, and nodules on the seafloor. Therefore, we deduce that the morphology of these mound-like structures may represent varying degrees of seepage intensity. The process of moderate natural gas seepage can lead to the formation of seafloor spiny seamounts. Gas accumulates within the shallow subsurface hydrate stability zone, and under suitable temperature and pressure conditions, it is prone to forming blocky or fissure-filling natural gas hydrates [34]. Low-speed natural gas seepage processes can lead to the formation of domed seamounts. Domed seamounts are often associated with carbonate rock substrates. Due to their well-developed fractures, they are prone to forming diffusive-type natural gas hydrates. The spiny seamounts associated with hydrates typically display an oval or concentric positive topography when viewed from above. The formation of these features is a result of the accumulation of free gas within sedimentary layers. This process involves gas generated by hydrate dissociation replacing the water in the pores of upper sediment layers, causing localized expansion and resulting in a positive topographic feature [35].

5.3. Potential Seafloor Seepage Patterns in the Study Area

In summary, this study proposes a seafloor seepage model for the southern QDNB (Figure 4).

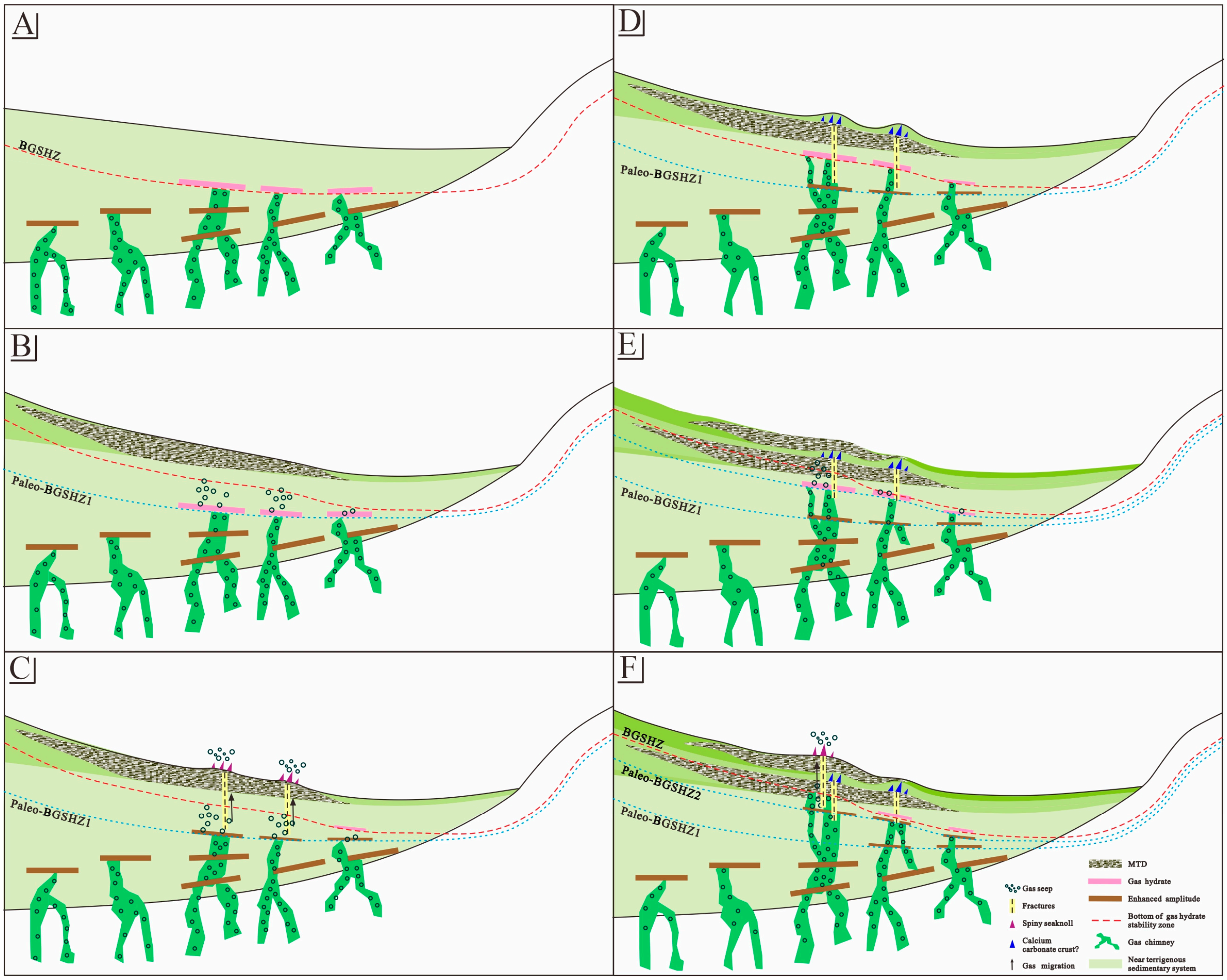

Figure 4. Seafloor seepage pattern in the study area.

Stage A. Influenced by tectonic activities since the Middle-Neogene, deep-seated fluids are released upward along tectonic weak zones characterized by developed fractures, forming vertical migration pathways primarily composed of gas chimneys. The Huangliu Formation offers favorable conditions for biogenic gas generation, as sedimentary rock layers contain adequate organic matter abundance, appropriate maturity, and temperature conditions. Biogenic gas migrates toward the hydrate stability zone through gas chimneys. The continuous biogenic gas supply, combined with the accumulation of in-situ microbial methane gas within the stability zone, leads to the formation of methane hydrates when the methane concentration reaches saturation. Simultaneously, as biogenic gas continues its upward migration and encounters highly permeable sedimentary layers, it can accumulate to form shallow gas reservoirs.

Stage B. With the rapid deposition of the first-phase MTDs, significant changes in temperature and pressure occur within the stability zone formed during Stage A in the MTD coverage area, leading to the decomposition of the original gas hydrate bodies and the release of a large amount of methane gas. This results in the decomposition of pre-existing hydrate deposits formed in Stage A and the release of a significant amount of methane gas. The central part of MTDs exhibits greater thickness, leading to a notable uplift of the BGHSZ and the release of a larger amount of methane gas. Conversely, the thinner flanks of MTDs experience less uplift of the BGHSZ, leading to the reduced release of methane gas.

Stage C. When the methane gas rapidly released from hydrate decomposition and the continuously supplied deep-seated fluids reach a certain level, they undergo overpressure release (Figure 4C). At this point, microfractures carrying fluids and sediment penetrate through the seafloor, resulting in the upward arching of the strata, spiny seamounts, and seafloor sediment folding. Due to the ongoing gas leakage, self-generated carbonate crusts and chemosynthetic biogenic shells form near the leakage points, leading to an expansion in the distribution and development range of spiny seamounts.

Stage D. As the high-level depositional regime experiences stable, uniform, and gradual subsidence, the temperature and pressure within the stability zone gradually stabilize, resulting in a slowdown in the rate of hydrate decomposition. With increasing sediment thickness, the BGHSZ gradually moves upward until it reaches a relatively stable position. At this point, the continuously supplied fluids will slowly form new hydrate bodies near the BGHSZ.

Stage E. With the rapid deposition of the latest MTDs, there is another rapid change in temperature and pressure within the stability zone. The BGHSZ formed during Stage D experiences rapid uplift, leading to the rapid decomposition of natural gas hydrate bodies.

Stage F. When the thickness of the most recent MTDs is substantial, the corresponding alteration of the BGHSZ is significant, leading to a higher rate of decomposition of hydrate bodies and stronger overpressure release. During this period, microfractures carrying fluids and sediment pierce the seafloor, alongside the ongoing gas leakage and expansion of gas hydrate mineralization. These factors contribute to the formation of more distinct underwater mounds and upward arching in the geological layers. On the other hand, when the thickness of the latest MTDs is thinner, there is relatively minimal alteration in the BGHSZ. After the decomposition of hydrates, the gas formed quickly re-mineralizes within a shorter vertical fissure in the new stable zone, without venting or leaking to the seafloor. Consequently, this process leads to the development of domed seamounts.

6. Conclusions

6.1. Impacts of MTDs on Seafloor Gas Seepage

The rapid sedimentation of MTDs leads to the swift alteration of the BGHSZ, triggering the substantial decomposition of hydrates and the release of a significant amount of natural gas. This gas migrates towards the seafloor and punctures through it, constituting the primary cause of varying degrees of seafloor seepage in the study area. In regions where MTDs are thicker, the uplift of the BGHSZ is more pronounced. Consequently, the speed of natural gas hydrate decomposition accelerates, resulting in a higher gas seepage rate and greater damage to the seafloor micro-features. Conversely, the opposite holds true.

6.2. Association of Seafloor Seamounts with Gas Seepage

It has been discovered that seafloor spiny seamounts and domed seamounts are closely associated with seafloor gas seepage. Spiny seamounts represent moderate-speed natural gas seepage in the shallow overburden, while domed seamounts signify slow-speed natural gas seepage in the same layer. The zones with dense development of fractures in the underlying formations of both types of mounds are ideal sites for leaky gas hydrates. They could potentially serve as crucial indicators for identifying leaky gas hydrates during exploration activities on the northern slope of the South China Sea.

Author Contributions: Writing—original draft preparation, P.L.; methodology, W.Z. and L.H.; validation, S.M. and H.C.; data curation, P.S. All authors have read and agreed to the published version of the manuscript.

Funding: We gratefully acknowledge the financial support provided by the National Science Foundation of China (42176215), the Guangzhou Science and Technology Planning Project (202201011434), the First Batch of the "Nanhai New Star" project (NHXXRCXM202357), the Guangdong Basic and Applied Basic Research Foundation (2019B030302004), Project of Sanya Yazhou Bay Science and Technology City (SCKJ-JYRC-2023-02), and Sanya Science and Technology Innovation Project (2022KJCX14).

Data Availability Statement: The data presented in this study are available on request from the corresponding author. The data are not publicly available due to legal restrictions.

Conflicts of Interest: Author Pengqi Liu was employed by Sanya Institute of South China Sea Geology, Guangzhou Marine Geological Survey. The remaining authors declare that the research was conducted in the absence of any commercial or financial relationships that could be construed as a potential conflict of interest.

References

1. Wang, B. Research on Typical Seabed Fluid Flows in China Marginal Seas. Ph.D. Dissertation, Chinese Academy of Sciences, Qingdao China, 2018.
2. Judd, A.; Hovland, M. *Seabed Fluid Flow Impact of Geology, Biology and the Marine Environment*; Great Britain at the Alden Press: Oxford, UK, 2007.
3. Ho, S.; Cartwright, J.A.; Imbert, P. Vertical evolution of fluid venting structures in relation to gas flux, in the Neogene-Quaternary of the Lower Congo Basin, Offshore Angola. *Mar. Geol.* **2012**, *332*, 40–55. [CrossRef]
4. Wang, J.; Wu, S.; Kong, X.; Ma, B.; Li, W.; Wang, D.; Gao, J.; Chen, W. Subsurface fluid flow at an active cold seep area in the Qiongdongnan Basin, northern South China Sea. *J. Asian Earth Sci.* **2018**, *168*, 17–26. [CrossRef]
5. Moore, G.F.; Saffer, D.; Studer, M.; Costa Pisani, P. Structural restoration of thrusts at the toe of the Nankai Trough accretionary prism off Shikoku Island, Japan: Implications for dewatering processes. *Geochem. Geophys. Geosyst.* **2011**, *12*. [CrossRef]
6. Goshovskyi, S. Gas seeps as the black sea hydrocarbon resource. *Int. Multidiscip. Sci. GeoConf. SGEM* **2019**, *19*, 877–882.
7. Bondarenko, V.; Ganushevych, K.; Sai, K.; Tyshchenko, A. Development of gas hydrates in the Black Sea. *Tech. Geoinformational Syst. Min.* **2011**, 55–59. Available online: https://www.researchgate.net/publication/330310759_Development_of_gas_hydrates_in_the_Black_sea (accessed on 4 March 2024).
8. Klymenko, V.; Ovetskyi, S.; Martynenko, V.; Vytiaz, O.; Uhrynovskyi, A. An alternative method of methane production from deposits of subaquatic gas hydrates. *Min. Miner. Depos.* **2022**, *16*, 11–17. [CrossRef]
9. Yang, C.; Li, X.; Yao, Y.; Chang, X.; Wu, J.; Huang, L.; Ju, D. The subsurface fluid-flow systems and their genetic mechanism in the southwestern barents sea. *Mar. Geol. Quat. Geol.* **2015**, *35*, 135–143.
10. Mark, C.; Srikumar, R.; Conor, O.; Annika, C.; Ronan, O.; Ruth, P. Geological settings and controls of fluid migration and associated seafloor seepage features in the north Irish Sea. *Mar. Pet. Geol.* **2021**, *123*, 104762.
11. Dugan, B.; Flemings, P.B. Overpressure and Fluid Flow in the New Jersey Continental Slope: Implications for Slope Failure and Cold Seeps. *Science* **2000**, *289*, 288–291. [CrossRef] [PubMed]
12. Crutchley, G.J.; Kroeger, K.F.; Pecher, I.A.; Gorman, A.R. How tectonic folding influences gas hydrate formation: New Zealand's Hikurangi subduction margin. *Geology* **2019**, *47*, 39–42. [CrossRef]
13. Doré, A.G.; Jensen, L.N. The impact of late Cenozoic uplift and erosion on hydrocarbon exploration: Offshore Norway and some other uplifted basins. *Glob. Planet. Chang.* **1996**, *12*, 415–436. [CrossRef]

14. Pape, T.; Blumenberg, M.; Reitz, A.; Scheeder, G.; Schmidt, M.; Haeckel, M.; Wallmann, K.; Bohrmann, G. Oil and gas seepage offshore Georgia (Black Sea)–Geochemical evidences for a Paleogene-Neogene hydrocarbon source rock. *Mar. Pet. Geol.* **2021**, *128*, 104995. [CrossRef]
15. Chen, J.; Song, H.; Guan, Y.; Pinheiro, L.M.; Geng, M. Geological and oceanographic controls on seabed fluid escape structures in the northern Zhongjiannan Basin, South China Sea. *J. Asian Earth Sci.* **2018**, *168*, 38–47. [CrossRef]
16. Bouchaala, F.; Guennou, C. Estimation of viscoelastic attenuation of real seismic data by use of ray tracing software: Application to the detection of gas hydrates and free gas. *C. R. Geosci.* **2012**, *344*, 57–66. [CrossRef]
17. Liang, J.Q.; Fu, S.Y.; Chen, F.; Su, P.; Shang, J.; Lu, H.; Fang, Y. Characteristics of methane seepage and gas hydrate reservoir in the northeastern slope of South China Sea. *Nat. Gas Geosci.* **2017**, *28*, 761–770.
18. Waite, W.F.; Santamarina, J.C.; Cortes, D.D.; Dugan, B.; Espinoza, D.N.; Germaine, J.; Jang, J.; Jung, J.W.; Kneafsey, T.J.; Shin, H.; et al. Physical properties of hydrate-bearing sediments. *Rev. Geophys.* **2009**, *47*. [CrossRef]
19. Chen, L.; Song, H. Geophysical features and identification of natural gas seepage in marine environment. *Prog. Geophys.* **2005**, *20*, 1067–1073.
20. Wan, Z.; Chen, C.; Liang, J.; Zhang, W.; Huang, W.; Su, P. Hydrochemical characteristics and evolution mode of cold seeps in the Qiongdongnan Basin, South China Sea. *Geofluids* **2020**, *2020*, 4578967. [CrossRef]
21. Zhao, Z.; Sun, Z.; Sun, L.; Wang, Z.; Sun, Z. Cenozoic tectonic subsidence in the Qiongdongnan basin, northern South China Sea. *Basin Res.* **2018**, *30*, 269–288. [CrossRef]
22. Hongfang, G.; Xin, N.; Weidong, L. Source to sink analysis of a sea basin: The Quaternary deepwater turbidite fan system in Pearl River Valley-Northwest subbasin, Northern South China Sea. *Mar. Geol. Quat. Geol.* **2021**, *41*, 1–12.
23. Lei, Z.; Su, M.; Zhang, L.; Shuai, Q.; Sun, M.; Liu, J.; Yang, R. Sediment sources and transport patterns of Qiongdongnan Basin in northern slope of South China Sea since late Miocene. *J. Mar. Sci.* **2016**, *34*, 35–42.
24. Pang, X. Sequence stratigraphy configuration of deepwater gravity-flow sediments and its controls: A line of thinking in sequence stratigraphy of gravity-flow sediments in Baiyun deepwater area, the northern South China Sea. *China Offshore Oil Gas* **2012**, *24*, 1–8.
25. Mao, S.; Hu, G.; Hu, L.; Liu, P.; Chen, X.; Qin, M.; Cheng, F. Evaluation of Natural Gas Hydrate Fault System: A Case from a Sag in Deep-Water Slope Area of the Northern South China Sea. *Lithosphere* **2022**, *2022*, 9049312. [CrossRef]
26. Taner, M.T.; Koehler, F.; Sheriff, R.E. Complex seismic trace analysis. *Geophysics* **1979**, *44*, 1041–1063. [CrossRef]
27. Bouchaala, F.; Ali, M.Y.; Matsushima, J.; Bouzidi, Y.; Takougang, E.T.; Mohamed, A.A.; Sultan, A.A. Scattering and intrinsic attenuation as a potential tool for studying of a fractured reservoir. *J. Pet. Sci. Eng.* **2019**, *174*, 533–543. [CrossRef]
28. Huang, Y.P.; Geng, J.H.; Zhong, G.F.; Guo, T.L.; Pu, Y.; Ding, K.Y.; Ma, J.Q. Seismic attribute extraction based on HHT and its application in a marine carbonate area. *Appl. Geophys.* **2011**, *8*, 125–133. [CrossRef]
29. Hart, B.S. Channel detection in 3-D seismic data using sweetness. *AAPG Bull.* **2008**, *92*, 733–742. [CrossRef]
30. Khan, N.; Khan, S.; Rehman, F.; Sajid, M. Structural and seismic attribute analysis of the Paleocene carbonate reservoir from the Balkassar Field, Potwar Plateau, Pakistan. *J. Pet. Res. Stud.* **2024**, *14*, 18–35.
31. Musgrave, R.J.; Bangs, N.L.; Larrasoaña, J.C.; Gràcia, E.; Hollamby, J.A.; Vega, M.E. Rise of the base of the gas hydrate zone since the last glacial recorded by rock magnetism. *Geology* **2006**, *34*, 117–120. [CrossRef]
32. Zhao, T.; Zhang, X.; Feng, J. Acoustic detection techniques for seabed hydrocarbon seepage. *Mar. Geol. Quat. Geol.* **2010**, *30*, 149–156.
33. Roberts, H.H.; Hardage, B.A.; Shedd, W.W.; Hunt, J., Jr. Seafloor reflectivity—An important seismic property for interpreting fluid/gas expulsion geology and the presence of gas hydrate. *Lead. Edge* **2006**, *25*, 620–628. [CrossRef]
34. Shang, J.; Wu, L.; Liang, J.; Sha, Z.B. The microtopographic features and gas seep model on the slope in the northeastern South China Sea. *Mar. Geol. Quat. Geol.* **2014**, *34*, 129–136.
35. Paull, C.K.; Normark, W.R.; Ussler III, W.; Caress, D.W.; Keaten, R. Association among active seafloor deformation, mound formation, and gas hydrate growth and accumulation within the seafloor of the Santa Monica Basin, offshore California. *Mar. Geol.* **2008**, *250*, 258–275. [CrossRef]